Optical absorption and photoluminescence in the defect-chalcopyrite-type semiconductor $ZnIn_2Te_4$

Shunji Ozaki, Sei-ichi Boku, and Sadao Adachi
Department of Electronic Engineering, Faculty of Engineering, Gunma University, Kiryu-shi, Gunma 376-8515, Japan
(Received 29 July 2003; published 1 December 2003)

Optical absorption and photoluminescence (PL) spectra have been measured on the defect-chalcopyrite-type semiconductor $ZnIn_2Te_4$ in the 1.1–1.6 eV photon-energy range at temperatures between 11 and 300 K. The temperature dependence of the direct-gap energy of $ZnIn_2Te_4$ has been determined from the optical absorption spectra and fit using the Varshni equation and an analytical four-parameter expression developed for the explanation of the band-gap shrinkage effect in semiconductors. The PL spectra show an asymmetric emission band at ~1.4 eV, which is attributed to donor-acceptor pair recombination between quasicontinuously distributed donor states and acceptor levels. At temperatures above 90 K, the band-to-band emission begins to appear at the high-energy tail of the donor-acceptor pair recombination. A double-exponential fit analysis of the PL spectra suggests an acceptor level of 64 meV and an unidentified shallow level of 9 meV. An energy-band scheme has been proposed for the explanation of PL emission in the defect-chalcopyrite-type semiconductors.

DOI: 10.1103/PhysRevB.68.235201 PACS number(s): 78.20.Ci, 78.40.Fy, 78.55.Hx

I. INTRODUCTION

The ternary semiconducting compounds, $A^{II}B^{III}{}_2C^{VI}{}_4$, have been widely investigated because of their potential applications to electrooptic, optoelectronic, and nonlinear optical devices.[1] Most of these compounds have defect chalcopyrite (space group $=S_4^2$) or defect stannite (space group $=D_{2d}{}^{11}$) structure.[2] In an $A^{II}B^{III}{}_2C^{VI}{}_4$ defect chalcopyrite compound, A, B, and C atoms and vacancy are distributed as follows:[3] A on $(a/2,0,c/4)$, B on $(0,0,c/2)$, $(0,a/2,c/4)$, C on $(\alpha,\overline{\beta},\gamma)$, $(\overline{\alpha},\beta,\gamma)$, $(\beta,\alpha,\overline{\gamma})$, $(\overline{\beta},\overline{\alpha},\overline{\gamma})$, and vacancy on (0,0,0). $ZnIn_2Te_4$ is one of the defect chalcopyrite family and is known to have an ideal chalcopyrite structure,[4] i.e., its lattice parameters are simply given by $\alpha=\beta=a/4$, $\gamma=c/8$, and $c=2a$. Although the material has been the subject of many research efforts, many fundamental properties are not sufficiently evaluated or are even unknown.[4]

Very little is known about the optical properties of $ZnIn_2Te_4$.[3,5–9] Boltivets *et al.*[7] used optical absorption and photoconductivity techniques to study the intrinsic absorption edge of $ZnIn_2Te_4$ and obtained a value of $E_g \sim 1.3$ eV at 300 K. Manca *et al.*[8,9] measured fundamental-reflectivity and photoconductivity spectra of polycrystalline $ZnIn_2Te_4$, and concluded that the material has an indirect gap near 1.40 eV (1.52 eV), as well as the lowest direct gap near 1.87 eV (1.90 eV) at 300 K (85 K). However, this conclusion was obtained relatively easily from the fact that direct transitions generate a peak only in reflectivity, while both direct and indirect transitions are responsible for photoconductivity. Manca *et al.*[8,9] also observed some reflectivity structures at energies ~2.2, ~2.4, and ~3.6 eV, but they gave no detailed discussion on these structures.

In our previous paper[3] we synthesized bulk polycrystalline $ZnIn_2Te_4$ and measured its pseudodielectric-function spectra by using spectroscopic ellipsometry. The measured pseudodielectric-function spectra revealed distinct structures at various critical points, and these structures were assigned to specific points in the Brillouin zone by the aid of a band-structure calculation using empirical pseudopotential method. Room-temperature optical absorption also showed that $ZnIn_2Te_4$ is a direct-gap semiconductor having the lowest-direct-gap energy at ~1.40 eV.

In this article, we present the optical absorption and photoluminescence (PL) spectra for $ZnIn_2Te_4$ measured at temperatures T between 11 and 300 K. The temperature dependence of the lowest-band-gap energy E_g for $ZnIn_2Te_4$ will be determined by the optical absorption measurements. The dependence of E_g on T is commonly described by the empirical equation proposed by Varshni.[10] A novel analytical expression has been recently proposed by Pässler[11,12] by considering the band-gap shrinkage effect in accordance with general equations and parameter relationships governing the electron-phonon interaction mechanism. The E_g versus T data for $ZnIn_2Te_4$ will be analyzed using these expressions. No PL measurement has been performed on $ZnIn_2Te_4$ to date. We will observe a single, asymmetric PL emission band at ~1.4 eV, which is attributed to transitions from the quasicontinuously distributed donor states below the conduction band to acceptor levels. The quasicontinuously distributed or exponentially tailed donor states may be caused by a large number of donors in the defect chalcopyrite or stannite semiconductors.[1,13]

II. EXPERIMENT

The $ZnIn_2Te_4$ crystals used were grown by the conventional Bridgman method reported in the previous work.[14] They were polycrystalline with grain size of several mm^3. The hot-probe measurements suggested that the electrical conductivity of the samples is p type. The samples were prepared by cutting the ingot with a wire saw, by mechanically polishing, and finally by chemically etching with a solution of Br_2 in methanol. Thickness of the samples was ~0.14 mm.

The halogen lamp was used for optical absorption measurements, and the 488.0 nm line of an Ar^+-ion laser (NEC GLG3110) chopped at 320 Hz was used as the excitation light source for PL measurements. The optical absorption and PL spectra were taken in the 1.1–1.6 eV photon-energy

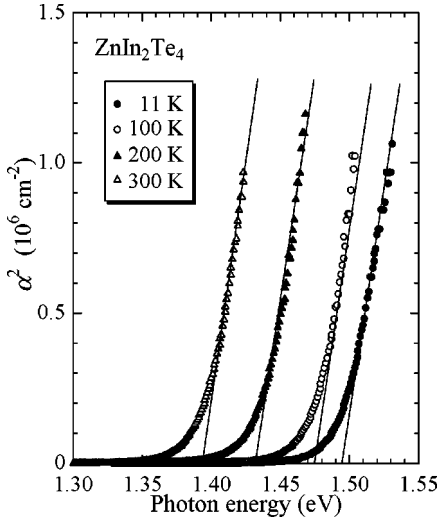

FIG. 1. Plots of the square of the absorption coefficient, α^2, versus photon energy for $ZnIn_2Te_4$ at $T=11-300$ K. The intercept point on the energy axis gives the band-gap energy E_g at each temperature.

range using a grating spectrometer (JASCO CT-25C) and a liquid-nitrogen cooled Ge photodiode (Hamamatsu B6175-05). The spectral resolution of the grating spectrometer used was about ± 0.1 nm (± 0.2 meV) at the band edge of $ZnIn_2Te_4$. The measurements were performed using a closed-cycle refrigerator cryostat (IWATANI CRT105PL) between $T=11$ and 300 K. Note that the experiments were carried out on a few grains of the polycrystalline sample. No attention was, therefore, paid to the polarization dependence of the optical spectra.

III. RESULTS AND DISCUSSION

A. Optical absorption measurements

One of the most important parameters characterizing semiconducting properties is the band-gag energy E_g. In order to determine the fundamental band-gap energy of $ZnIn_2Te_4$, we measured optical absorption spectra of the material. The absorption coefficient α was determined from the experimental transmittance T using the relation

$$T=\frac{(1-R)^2e^{-\alpha x}}{1-R^2e^{-2\alpha x}}, \tag{1}$$

where R is the reflectivity. We used a value of $R=0.25$ which was obtained from our previous spectroscopic ellipsometry data.[3]

The experimental absorption spectra measured at $T=11-300$ K for $ZnIn_2Te_4$ are shown in Fig. 1. The dependence of α on photon energy E can be written as

$$\alpha(E)=A(E-E_g)^n, \tag{2}$$

or, equivalently

$$\alpha(E)^{1/n}=A^{1/n}(E-E_g), \tag{3}$$

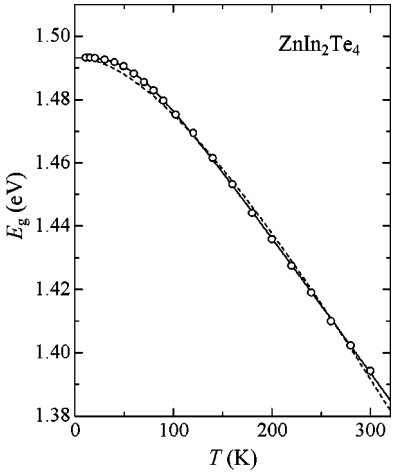

FIG. 2. Plots of E_g versus T for $ZnIn_2Te_4$ determined from the optical absorption measurements. The dashed and solid lines represent the calculated results of Eqs. (4) and (5), respectively. The fit-determined parameters are listed in Table I.

where $n=1/2$ and 2 correspond to the direct and indirect band gaps, respectively. We found that the fit is superior for $n=1/2$ than for 2. This fact suggests that $ZnIn_2Te_4$ may be a direct-gap semiconductor.[3] The plots in Fig. 1 give intercepts, $E_g \sim 1.49$ eV ($T=11$ K), ~ 1.48 eV ($T=100$ K), ~ 1.44 eV ($T=200$ K), and ~ 1.39 eV ($T=300$ K), on the energy axis.

Traditionally, temperature variation of the band-gap energy is expressed in terms of Varshni's formula[10]

$$E_g(T)=E_g(0)-\frac{\alpha T^2}{T+\beta}, \tag{4}$$

where $E_g(0)$ is the band-gap energy at $T=0$ K, α is in electron volts per degree Kelvin, and β is closely related to the Debye temperature of the material (in Kelvins). The dashed line in Fig. 2 represents the least-squares fit of the experimental data to Eq. (4). The fit-determined parameter values are listed in Table I.

Recently, Pässler[11,12] proposed an analytical expression which takes into account the band-gap shrinkage effect in accordance with general equations and parameter relationships governing the electron-phonon interaction mechanism:

$$E_g(T)=E_g(0)-\frac{\alpha_p\Theta_p}{2}\left[\sqrt[p]{1+\left(\frac{2T}{\Theta_p}\right)^p}-1\right], \tag{5}$$

where α_p plays the role of a $T\rightarrow\infty$ limiting value of the band-gap shrinkage coefficient $-\partial E_g(T)/\partial(T)$, Θ_p is approximately equal to the average phonon temperature, and the power exponent p is closely related to the overall shape of the electron-phonon spectral function in the given material. This expression is more palatable than Eq. (4) from the theoretical point of view. The solid line in Fig. 2 indicates the fitted result of the data to Eq. (5). The fit-determined parameters are listed in Table I. We can see in Fig. 2 that Eq. (5) shows a better agreement with the experimental data in the $T=15-300$ K temperature range compared with Eq. (4).

TABLE I. Values of $E_g(0)$, α, and β in Eq. (4) and those of α_p, Θ_p, and p in Eq. (5) for $ZnIn_2Te_4$.

$E_g(0)$ (eV)	α (meV/K)	β (K)	α_p (meV/K)	Θ_p (K)	p
1.493	0.60	235	0.43	138	3.2

The effective phonon temperature Θ_p in Eq. (5) is expected to be related to the Debye temperature θ_D by $\Theta_p \sim 2/3\theta_D$.[11] The Θ_p value listed in Table I is 138 K. We can, thus, obtain $\theta_D \sim 207$ K for $ZnIn_2Te_4$. No θ_D value has been reported for $ZnIn_2Te_4$. We can, however, find that the estimated value of $\theta_D \sim 207$ K is slightly smaller or larger than the ZnTe values of $\theta_D \sim 228$ K (Ref. 15) and $\sim 190 \pm 20$ (Ref. 16) at $T=0$ K, respectively, and is smaller than the ZnTe value of $\theta_D \sim 260$ K at $T=300$ K (Ref. 17). We find, from a plot of the Debye temperature θ_D versus lattice parameter a for some group-IV, III–V, and II–VI semiconductors, the relation between θ_D and a given by $\ln \theta_D = 10.53 - 0.834a$ (a in Å; θ_D in K). This relation provides $\theta_D \sim 249$ K for ZnTe ($a=6.01$ Å) and $\theta_D \sim 229$ K for $ZnIn_2Te_4$ ($a=6.11$ Å, Ref. 4). The above estimated θ_D values of ~ 207 K and ~ 229 K for $ZnIn_2Te_4$ are also found to be nearly equal to the characteristic temperature of $\beta \sim 235$ K in Eq. (4) (Table I). Furthermore, this characteristic temperature ($\beta \sim 235$ K) is nearly equal to an effective longitudinal optical (LO) phonon temperature $\theta \sim 284$ K obtained from the relation of $k\theta = \hbar\omega_{LO}$ (~ 24.5 meV, Ref. 5). The latter fact suggests that the major contribution to the temperature variation of E_g in $ZnIn_2Te_4$ is apparently due to the optical phonons.

Differentiating Eq. (5) with respect to T, we obtain

$$\frac{\partial E_g(T)}{\partial T} = -\alpha_p \left(\frac{2T}{\Theta_p}\right)^{p-1} \left[1+\left(\frac{2T}{\Theta_p}\right)^{p}\right]^{(1-p)/p}. \qquad (6)$$

The temperature coefficient $\partial E_g/\partial T$ for $ZnIn_2Te_4$ at $T=300$ K obtained from Eq. (6) is -0.43 meV/K. Manca *et al.*[9] reported the $\partial E_g/\partial T$ value for $ZnIn_2Te_4$ to be -0.6 meV/K. This value was, however, estimated from their measured photoconductivity peaks by assuming that E_g has the same temperature dependence as the photoconductivity peak energy. We can also point out that our obtained $\partial E_g/\partial T$ value is very close to that for ZnTe (-0.45 meV/K)[18] but is much smaller than that for In_2Te_3 (-0.59 meV/K).[19]

B. PL measurements

Figure 3 plots the PL spectra obtained for $ZnIn_2Te_4$ at temperatures between 11 and 300 K. The arrow indicates the position of the band-gap energy E_g at each temperature. It is evident from Fig. 3 that at low temperatures the PL spectra show a single, broad emission band peaking at ~ 1.4 eV. At higher temperatures than ~ 90 K, a new emission band appears at the high-energy side of the ~ 1.4-eV emission band (see Fig. 4, below). Note that the single, broad emission band observed at low temperatures is strongly asymmetric with tail at the low photon-energy side. This type of luminescence band has been commonly observed in such $II-III_2-VI_4$ defect chalcopyrite or stannite semiconductors such as $ZnGa_2Se_4$,[20] $ZnIn_2S_4$,[21] $CdGa_2Se_4$,[22] $CdIn_2S_4$,[23,24] and $CdIn_2Te_4$ (Ref. 25) (see also Refs. 1 and 13).

In order to explain the observed PL spectra, we consider that the density of states in the conduction-band tail depends exponentially on the energy distance from the unperturbed conduction-band edge[21]

$$N_D(E) = \begin{cases} N_D^0 \exp[m(E-E_d)], & E \leqslant E_d, \\ 0, & E > E_d, \end{cases} \qquad (7)$$

where E_d is the so-called "demarcation level" of the donor band and m is the slope of the conduction-band tail. The slope parameter m is assumed to be independent of T. The exponential donor states may arise from the failure in the periodic distribution of the stoichiometric voids in the defect chalcopyrite structure.[13] Anedda *et al.*[26] measured the photoconductivity of $CdIn_2S_4$ and found a high density ($\sim 10^{20}$ cm^{-3}) of electron trap levels with an exponential distribution in energy. They explained such higher density electron traps in terms of higher disorder in the cation sublattice. The same electron traps as in $CdIn_2S_4$ have been observed in $ZnIn_2Te_4$ (Ref. 9) and other isostructural $A^{II}B_2^{III}C_4^{VI}$ crystals.[1,13]

The acceptor states are assumed to exhibit a broadened Gaussian distribution given by

$$N_A(E) = N_A^0 \exp\left[-\frac{(E-E_A)^2}{\Gamma^2}\right], \qquad (8)$$

where N_A^0 is the acceptor concentration, E_A is the acceptor ionization energy, and Γ is the broadening parameter of the acceptor states.

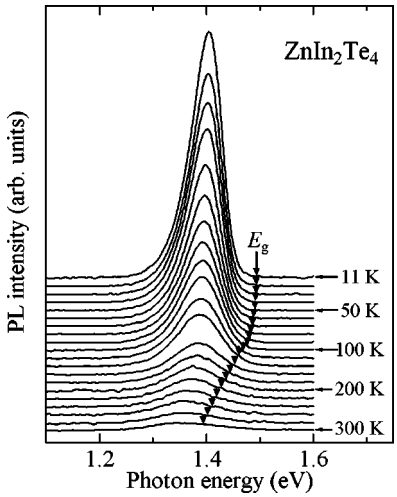

FIG. 3. PL spectra of $ZnIn_2Te_4$ measured at $T=11-300$ K. The vertical arrows indicate the positions of the band-gap energy E_g.

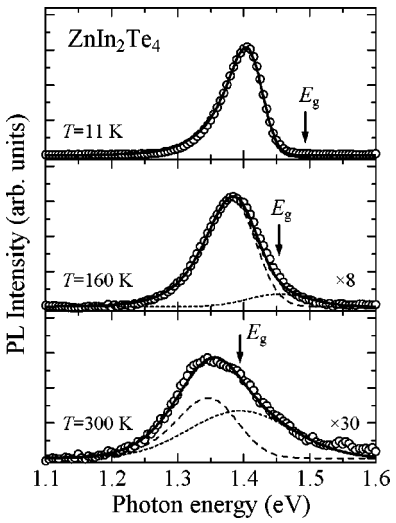

FIG. 4. Theoretical fits of the PL spectra $I(E,T)$ for $ZnIn_2Te_4$ measured at $T=11$, 160, and 300 K. The dashed and dotted lines represent the DA pair (I_{DA}) and band-to-band emission components (I_{BB}) obtained from Eqs. (10) and (11), respectively, while the heavy solid line indicates the sum of these components. The vertical arrows indicate the positions of the band-gap energy E_g.

The temperature dependence of the integrated PL intensity for the ~1.4-eV peak did not show a simple exponential behavior, $\exp(E_A/kT)$, defined by an activation energy E_A of the acceptor states. We found that the experimental results can be well explained by a double-exponential fit.[27] Note that the photogenerated carrier distribution in localized states cannot be described by thermal equilibrium conditions. Therefore, we modify Eq. (8) by taking into account the double-exponential fit model as[27]

$$N_A(E,T)=\frac{N_A^0}{1+Ae^{-E_A/kT}+Be^{-E_X/kT}}\exp\left[-\frac{(E-E_A)^2}{\Gamma^2}\right]. \tag{9}$$

The donor-acceptor (DA) recombination emission intensity $I_{DA}(E,T)$ can be finally given by the convolution integral as[21]

$$I_{DA}(E,T)=P\int N_A(E',T)N_D(E'+E)dE', \tag{10}$$

where P is the DA pair transition probability which is assumed to be independent of E and T. The parameters Γ and E_d influence essentially the peak width and asymmetry of the spectrum, respectively. The m value to be fit-determined below is 26.7 eV^{-1}.

Figure 4 shows the fitted results of the PL spectra $I(E,T)$ with Eq. (10) measured at $T=11$, 160, and 300 K. It is clear from Fig. 4 that the experimental $I(E,T)$ spectrum at $T=11$ K shows excellent agreement with our theoretical calculation; however, no good agreement can be found between the experimental and calculated spectra for $T=160$ and 300 K. In order to improve the fit, therefore, we consider an additional contribution that is caused by the band-to-band emission. The spectrum of the band-to-band emission can be modeled using a Gaussian line shape as

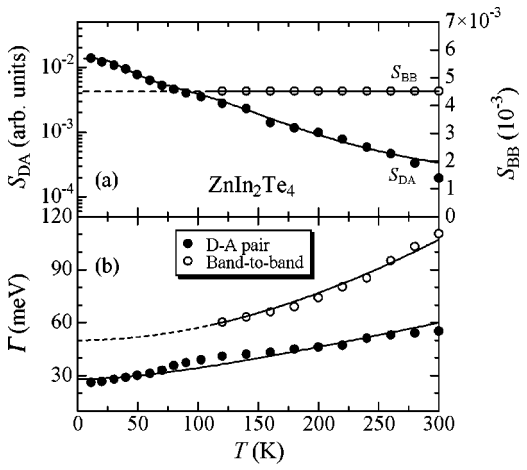

FIG. 5. (a) Temperature variation of the strength parameters for the DA pair (S_{DA}) and band-to-band emissions (S_{BB}) in $ZnIn_2Te_4$. The solid line (S_{DA}) shows the calculated result of Eq. (12). (b) Temperature variation of the broadening parameters Γ for the DA pair and band-to-band emissions for $ZnIn_2Te_4$. The solid lines show the calculated results of Eq. (14).

$$I_{BB}(E,T)=S_{BB}\exp\left[-\frac{(E-E_g)^2}{\Gamma^2}\right]. \tag{11}$$

The contribution to $I(E,T)$ of the band-to-band emission $I_{BB}(E,T)$ is shown in Fig. 4 by the dotted lines. We can see that by considering this term, the fits with the experimental data at $T=160$ and 300 K can be greatly improved, as indicated by the heavy solid lines in Fig. 4.

The temperature-dependent strength parameter of the DA pair emission can be represented from Eqs. (7)–(10) as

$$S_{DA}(T)=\frac{S_{DA}^0}{1+Ae^{-E_A/kT}+Be^{-E_X/kT}}, \tag{12}$$

with

$$S_{DA}^0=N_D^0N_A^0P. \tag{13}$$

In Fig. 5(a), we show the variation of $S_{DA}(T)$ as a function of temperature T for $ZnIn_2Te_4$. The solid line represents the calculated result of Eq. (12) with $S_{DA}^0=1.37\times10^{-2}$, $A=421$, and $B=6.6$. The activation energies determined here are $E_A=64$ meV and $E_X=9$ meV, respectively. The band-to-band strength parameter $S_{BB}(T)$ in Eq. (11) is also plotted against T in Fig. 5(a). It is found that S_{BB} can be satisfactorily approximated to be independent of T.

The broadening parameters Γ in Eqs. (9) and (11) versus T are shown in Fig. 5(b). The solid lines represent the best-fit results using an expression based on the Varshni's equation of Eq. (4):

$$\Gamma(T)=\Gamma(0)+\frac{\alpha_\Gamma T^2}{T+\beta_\Gamma}, \tag{14}$$

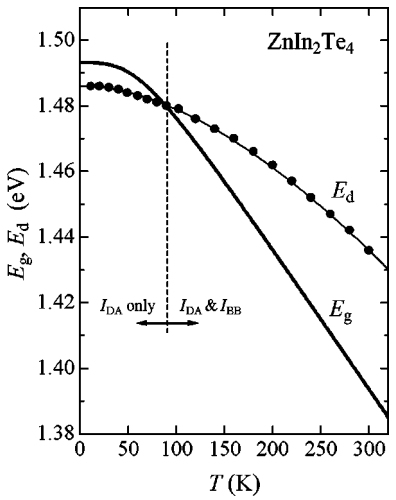

FIG. 6. Variation of the ''demarcation level'' width E_d as a function of temperature T for $ZnIn_2Te_4$. For comparison, the temperature variation of E_g is shown by the heavy solid line. The band-to-band emission I_{BB} appears only when $E_d > E_g$ ($T > 90$ K).

where $\Gamma(0)$ is the $T=0$ K value, α_Γ is in eV per degree Kelvin, and β_Γ is a characteristic temperature (in Kelvins). The parameter values determined here are $\Gamma(0)=28$ meV (50 meV), $\alpha_\Gamma = 1.6\times10^{-4}$ eV/K (1.14×10^{-3} eV/K), and $\beta_\Gamma = 150$ K (1500 K) for the DA pair (band-to-band) emission. The characteristic temperature $\beta_\Gamma = 150$ K for the DA pair emission corresponds to an effective phonon energy $\hbar\omega_q = k\theta \sim 13$ meV. This value is considerably smaller than the LO phonon energy of 24.5 meV for $ZnIn_2Te_4$.[5] This fact suggests that the major contribution to the lifetime broadening of the DA pair emission is due to acoustic phonons. On the other hand, the characteristic temperature $\beta = 1500$ K ($\hbar\omega_{q,\mathrm{eff}} = k\theta \sim 130$ meV) for the band-to-band emission is much larger than the LO phonon energy, $\hbar\omega_{LO} = 24.5$ meV. We can, thus, consider that the broadening parameter Γ in the band-to-band emission accounts for the distribution of the electronic states rather than being the consequence of its original concept (i.e., phonon and/or disorder lifetime broadening). In fact, the band-to-band emission can be observed only when the uppermost edge of the exponentially tailed donor levels crosses the conduction band (see Figs. 6 and 8, below).

Figure 6 shows the ''demarcation level'' width E_d plotted against temperature T for $ZnIn_2Te_4$. For comparison, the temperature dependence of E_g is plotted by the heavy solid line. As similar to E_g, E_d decreases with increasing T. However, its temperature change is found to be considerably smaller than that of E_g. As a result, a crossover occurs between E_g and E_d at $T \sim 90$ K. Our PL analysis did not require the band-to-band contribution I_{BB} at $T \leqslant 90$ K, but required it at T above 90 K. It is, thus, considered that for $T > 90$ K ($E_d > E_g$) a part of the donor electrons in the demarcation levels can be transferred to the conduction band, resulting in an appearance of the band-to-band emission.

The PL spectra measured at $T \leqslant 90$ K showed only the broad asymmetric emission band peaking at ~ 1.4 eV (i.e., well below the band-gap energy E_g). In order to confirm the

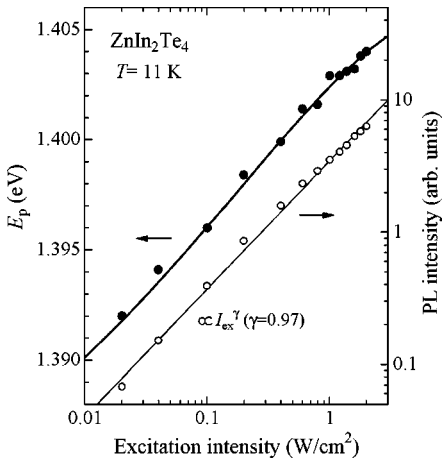

FIG. 7. Excitation intensity dependence of the PL peak energy (E_p) and integrated PL intensity for $ZnIn_2Te_4$ measured at $T = 11$ K. The heavy and light solid lines show the calculated results of Eqs. (15) and (16), respectively.

~ 1.4-eV emission band as actually due to the DA pair emission, we examined the excitation intensity dependence of the PL peak energy and integrated emission intensity at $T = 11$ K. Figure 7 presents the results of these experiments. It is found that the PL peak energy increases from 1.392 to 1.404 eV as the laser intensity increases from 0.02 to 2 W/cm^2. For the DA pair recombination, the excitation laser power I_{ex} can be expressed, as a function of PL peak energy E_p, as[28]

$$I_{ex} = I_0 \frac{(E_p - E_\infty)^3}{(E_B - E_\infty - 2E_p)} \exp\left(-\frac{2(E_B - E_\infty)}{E_p - E_\infty}\right), \qquad (15)$$

where I_0 is a proportionality constant, E_B is the emitted photon energy of a close DA pair separated by a shallow impurity Bohr radius, and E_∞ is the emitted photon energy of an infinity distant DA pair. The heavy solid line in Fig. 7 represents the fitted result of the experimental E_p values to Eq. (15). The fit-determined parameters are $E_B = 1.45$ eV and $E_\infty = 1.36$ eV. We can find that these parameters indeed satisfy the DA pair emission requirement of $E_\infty \leqslant E_p = 1.392 - 1.404$ eV $\leqslant E_B$.

The integrated PL intensity I versus I_{ex} can be given by the simple power law[28]

$$I \propto I_{ex}^{\gamma}. \qquad (16)$$

The dimensionless exponent γ is known to be $1 < \gamma < 2$ for free-exciton or bound-exciton emission and $\gamma \leqslant 1$ for free-to-bound or DA pair emission. The light solid line in Fig. 7 represents the fitted result of the experimental data to Eq. (16). The obtained value of $\gamma = 0.97$ supports an assignment of the 1.4 eV PL to DA pair recombination.

Finally, we show in Fig. 8 the schematic energy-band diagrams and PL emissions observed in $ZnIn_2Te_4$ for (a) $T = 11$ K, (b) 90 K, and (c) 300 K. The conduction-band and valence-band densities of states can be represented by the well-known expressions of $N_C \propto (E - E_C)^{1/2}$ and $N_V \propto (E_V - E)^{1/2}$, respectively. The exponentially tailed donor states of

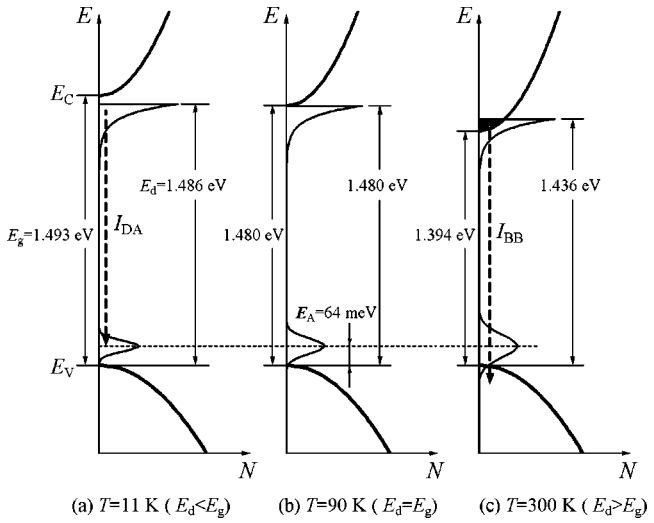

FIG. 8. Proposed energy-band scheme and electronic transitions in $ZnIn_2Te_4$ at (a) $T=11$ K, (b) 90 K, and (c) 300 K. The band-to-band emission I_{BB} appears only when $E_d>E_g$ ($T>90$ K).

Eq. (7) and broadened Gaussian-like acceptor states of Eq. (9) are also plotted in Fig. 8. The acceptor levels determined here are centered at 64 meV above the top of the valence band (E_A). The double-exponential quenching behavior of the I_{DA} emission suggests the presence of another impurity or trap level with an activation of $E_X=9$ meV. We could not, however, give an assignment whether it is an acceptorlike or a donorlike level.

The PL band caused by transitions from the exponentially tailed donor states to the broadened Gaussian acceptor levels showed the typical DA pair recombination characteristics, as seen in Fig. 7. It is easy to consider that in the vacancy tetrahedral semiconductors like $ZnIn_2Te_4$ the vacancies in the cation sublattice are the origin of the exponentially tailed donor states and Gaussian-like acceptor levels.[26] The photogenerated electrons in the conduction band can be efficiently transferred, via energy relaxation, to the exponentially tailed donor states. The donor-related emission is, thus, the dominant PL mechanism in $ZnIn_2Te_4$, and has been observed at all temperatures investigated ($T=11-300$ K). Reflecting the exponentially tailed donor states, the observed DA emission band is strongly asymmetric with tail at the low photon-energy side.

Both E_g and E_d decrease with increasing T, but they have clearly different temperature dependences that result in a change of their energy order at $T\sim90$ K. At T above 90 K (i.e., $E_d>E_g$), the band-to-band emission I_{BB} tends to appear at the high-energy side of the main I_{DA} peak. As seen in Fig. 8(c), an intermixing of the exponential donor and conduction-band states is the cause of the appearance of the band-to-band emission.

IV. CONCLUSIONS

We have measured the optical absorption and PL spectra on the defect-chalcopyrite-type ternary semiconductor $ZnIn_2Te_4$ in the 1.1–1.6 eV photon-energy range at $T=11-300$ K. The temperature dependence of the lowest-direct-gap energy E_g has been fit using two individual models. The PL spectra have been shown to originate from transitions between the quasicontinuously distributed donor states and acceptor levels located at 64 meV above the top of the valence band. A change in energy order between E_g and E_d (donor ''demarcation level'' width) is observed to occur at $T\sim90$ K. At above 90 K ($E_d>E_g$), the band-to-band emission tends to appear at the high-energy tail of the donor-acceptor pair emission, due to an intermixing between the quasicontinuously distributed donor and conduction-band states.

[1] A. N. Georgobiani, S. I. Radautsan, and I. M. Tiginyanu, Fiz. Tekh. Poluprovodn. (S.-Peterburg) **19**, 193 (1985) [Sov. Phys. Semicond. **19**, 121 (1985)].
[2] H. Hahn, G. Frank, W. Klingler, A. D. Störger, and G. Störger, Z. Anorg. Allg. Chem. **279**, 241 (1955).
[3] S. Ozaki and S. Adachi, Phys. Rev. B **64**, 085208 (2001).
[4] O. Madelung, in *Landolt-Börnstein: Numerical Data and Functional Relationships in Science and Technology*, edited by O. Madelung (Springer, Berlin, 1985), Vol. 17h.
[5] H. Neumann, W. Kissinger, F. Lévy, H. Sobotta, and V. Riede, Cryst. Res. Technol. **25**, 841 (1990).
[6] H. Neumann, W. Kissinger, and F. Lévy, Cryst. Res. Technol. **25**, 1189 (1990).
[7] N. S. Boltivets, V. P. Drobyazko, and V. K. Mityurev, Fiz. Tekh. Poluprovodn. (S.-Peterburg) **2**, 1037 (1968) [Sov. Phys. Semicond. **2**, 867 (1969)].
[8] P. Manca, F. Raga, and A. Spiga, Phys. Status Solidi A **16**, K105 (1973).
[9] P. Manca, F. Raga, and A. Spiga, Nuovo Cimento Soc. Ital. Fis., B **19**, 15 (1974).
[10] Y. P. Varshni, Physica (Amsterdam) **34**, 149 (1967).
[11] R. Pässler, Phys. Status Solidi B **200**, 155 (1997).
[12] R. Pässler, Phys. Status Solidi B **216**, 975 (1999).
[13] M. Guzzi and E. Grilli, Mater. Chem. Phys. **11**, 295 (1984).
[14] Y. Matsumoto, S. Ozaki, and S. Adachi, J. Appl. Phys. **86**, 3705 (1999).
[15] See H. Siethoff and K. Ahlborn, Phys. Status Solidi B **190**, 179 (1995).
[16] K. S. Gavrichev, G. A. Sharpataya, V. N. Guskov, J. H. Greenberg, T. Feltgen, M. Fiederle, and K. W. Benz, Phys. Status Solidi B **229**, 133 (2002).
[17] Estimated from data by D. N. Talwar, M. Vandevyver, K. Kunc, and M. Zigone, Phys. Rev. B **24**, 741 (1981).
[18] V. V. Sobolev, V. I. Donetskikh, and E. F. Zagaĭnov, Fiz. Tekh. Poluprovodn. (S.-Peterburg) **12**, 1089 (1978) [Sov. Phys. Semicond. **12**, 646 (1978)].
[19] O. H. Hughes, P. M. Nikolić, C. J. Doran, and S. S. Vujatović, Phys. Status Solidi B **71**, 105 (1975).
[20] S. I. Radautsan, I. M. Tiginyanu, V. N. Fulga, and Yu. O. Derid,

Phys. Status Solidi A **114**, 259 (1989).
[21] E. Grilli, M. Guzzi, E. Camerlenghi, and F. Pio, Phys. Status Solidi A **90**, 691 (1985).
[22] G. B. Abdullaev, V. G. Agaev, V. B. Antonov, R. Kh. Nai, and É. Yu. Salaev, Fiz. Tekh. Poluprovodn. (S.-Peterburg) **6**, 1729 (1972) [Sov. Phys. Semicond. **6**, 1492 (1973)].
[23] E. Grilli, M. Guzzi, P. Cappelletti, and A. V. Moskalonov, Phys. Status Solidi A **59**, 755 (1980).
[24] S. Charbonneau, E. Fortin, and J. Beauvais, Can. J. Phys. **65**, 204 (1987).
[25] G. Couturier, B. Jean, and J. Salardenne, J. Appl. Phys. **78**, 5654 (1995).
[26] A. Anedda, L. Garbato, F. Raga, and A. Serpi, Phys. Status Solidi A **50**, 643 (1978).
[27] M. R. Correia, S. Pereira, A. Cavaco, E. Pereira, and E. Alves, Appl. Phys. Lett. **80**, 4504 (2002).
[28] N. M. Gasanly, A. Serpengüzel, A. Aydinli, O. Gürlü, and I. Yilmaz, J. Appl. Phys. **85**, 3198 (1999).